Isotopes in Environmental and Health Studies, 2016
Vol. 52, Nos. 1–2, 75–93, http://dx.doi.org/10.1080/10256016.2015.1032961

Multiple sulphur and oxygen isotopes reveal microbial sulphur cycling in spring waters in the Lower Engadin, Switzerland

Harald Strauss[a*], Hannah Chmiel[a,b], Andreas Christ[a], Artur Fugmann[a], Kurt Hanselmann[c], Andreas Kappler[d], Paul Königer[e], Andreas Lutter[a], Katharina Siedenberg[a] and Barbara M.A. Teichert[a]

[a]*Institut für Geologie und Paläontologie, Westfälische Wilhelms-Universität Münster, Münster, Germany;* [b]*Limnology Department, Uppsala University, Uppsala, Sweden;* [c]*Department of Earth Sciences, Geomicrobiology Group, ETHZ, Zürich, Switzerland;* [d]*Geomicrobiology, Center for Applied Geosciences, University of Tuebingen, Tuebingen, Germany;* [e]*Bundesanstalt für Geowissenschaften und Rohstoffe, Hannover, Germany*

(*Received 2 October 2014; accepted 23 February 2015*)

Dedicated to Professor Dr Jochen Hoefs on the occasion of his 75th birthday

Highly mineralized springs in the Scuol-Tarasp area of the Lower Engadin and in the Albula Valley near Alvaneu, Switzerland, display distinct differences with respect to the source and fate of their dissolved sulphur species. High sulphate concentrations and positive sulphur ($\delta^{34}S$) and oxygen ($\delta^{18}O$) isotopic compositions argue for the subsurface dissolution of Mesozoic evaporitic sulphate. In contrast, low sulphate concentrations and less positive or even negative $\delta^{34}S$ and $\delta^{18}O$ values indicate a substantial contribution of sulphate sulphur from the oxidation of sulphides in the crystalline basement rocks or the Jurassic sedimentary cover rocks. Furthermore, multiple sulphur ($\delta^{34}S$, $\Delta^{33}S$) isotopes support the identification of microbial sulphate reduction and sulphide oxidation in the subsurface, the latter is also evident through the presence of thick aggregates of sulphide-oxidizing *Thiothrix* bacteria.

Keywords: hydrogen-2; isotope geochemistry; microbial sulphur cycling; oxygen-18; spring water; sulphate reduction; sulphur-33; sulphur-34; sulphur-36

1. Introduction

Numerous cold, mineralized springs, exhibiting electrical conductivities well above $1000\,\mu S\,cm^{-1}$, are situated in crystalline as well as sedimentary rocks in the Lower Engadin, the Albula Valley, and the Hinterrhein Valley, Switzerland. They include carbonate-, sulphur- and iron-rich springs [1–3]. These springs formed the basis for an extensive spa culture that flourished in the nineteenth and early twentieth centuries but continues to be of economic importance also today (www.graubuenden.ch).

In general, stable isotopes have been used successfully in hydrogeological/environmental studies, both with respect to reconstructing the water cycle as well as tracing the source and fate of dissolved constituents such as sulphate (e.g. [4]). Distinctly different isotope signatures characterize the potential sources of dissolved sulphate in surface waters and in groundwater (e.g.

*Corresponding author. Email: hstrauss@uni-muenster.de

[5–9]). Sulphate sources include the dissolution of evaporites, generally exhibiting positive $\delta^{34}S$ (e.g. [10–12]) and $\delta^{18}O$ values (e.g. [13]), or the oxidation of sulphide minerals in sedimentary rocks, exhibiting highly variable, yet frequently negative $\delta^{34}S$ values (e.g. [14,15]) or in igneous rocks, displaying a limited variability around a $\delta^{34}S$ value of 0 ‰ (e.g. [16]). The oxygen isotopic composition of sulphate resulting from sulphide oxidation can in principle be quite variable, depending upon the oxygen source, that is, atmospheric oxygen with a $\delta^{18}O$ value of + 23.5 ‰ [17,18] versus oxygen from meteoric water showing a generally negative $\delta^{18}O$ value [19,20]. Recent experimental studies [21,22] on the oxygen isotopic composition expressed during abiotic and/or biotic pyrite oxidation revealed that essentially all of the oxygen was derived from the water molecule. In contrast, recent river studies [5,7] revealed a more heterogeneous oxygen isotopic composition for pyrite-derived sulphate, suggesting a mixing between both principle sulphate oxygen sources and a dependence upon the principal oxidation pathway, that is, oxidation via molecular oxygen or via trivalent iron.

Microbial sulphur cycling is associated with in some cases substantial kinetic isotope fractionations of the stable sulphur isotopes (e.g. [15,23]). It has long been known that dissimilatory sulphate reduction, a process performed by strictly anaerobic sulphate-reducing bacteria, results in the depletion of ^{34}S in the reaction product hydrogen sulphide, leaving the remaining dissolved sulphate enriched in ^{34}S [15,24,25]. Numerous studies have shown that the residual sulphate is also enriched in ^{18}O [26], making the paired analysis of sulphur and oxygen isotopes a rather powerful tool for reconstructing microbial turnover of sulphate, for example, in groundwater studies. More recent studies have expanded sulphur isotope research towards the minor sulphur isotopes ^{33}S and ^{36}S (e.g. [23,27]), also expanding the possibilities for identifying distinct microbial processes. In contrast to sulphate reduction, microbial oxidation of sulphide is associated only with a minor, yet distinct, sulphur isotope effect (e.g. [28,29]). Finally, a third group of microbially mediated turnover of sulphur compounds of intermediate valence, such as elemental sulphur, sulphite, or thiosulphate, collectively termed disproportionation, is also associated with the isotopic fractionation of sulphur [30,31]. In conclusion, the application of multiple stable sulphur isotope analyses has been shown to advance our ability for reconstructing the different processes of microbial sulphur cycling (e.g. [29,32]).

This study focuses on selected springs located in the Lower Engadin, the Albula Valley, and at Rothenbrunnen (Hinterrhein Valley) with the emphasis placed on the source and fate of dissolved sulphate. In this study, we have applied sulphur and oxygen isotopes in order to link the dissolved sulphate of individual springs to the local bed rock. This includes the study of relevant rock samples and their sulphur isotopic composition. Moreover, multiple sulphur isotopes reveal microbially mediated sulphur cycling in the subsurface and at the surface discharge area.

2. Geological setting

The mineralized springs studied here are located in the Lower Engadine Valley in the Canton of Grisons (Graubünden), in the eastern Swiss Alps (Figure 1). The alpine orogeny provides the overall geological framework. On a more regional scale, the mineralized springs are located in the Engadine tectonic window, where the Austroalpine overthrusts have been eroded and the underlying Penninic rocks, comprising Jurassic oceanic crustal rocks and overlying sedimentary rocks, have become exposed (Figure 2). Consequently, deeply circulating waters (cf. [2,3]) have interacted with and are being discharged from lithologically variable rock units, comprising crystalline basement rocks as well as sedimentary rocks.

The springs studied in the Lower Engadine are located close to a major fault zone that runs through the Engadine Valley in the NE–SW direction. The surrounding crystalline rocks belong

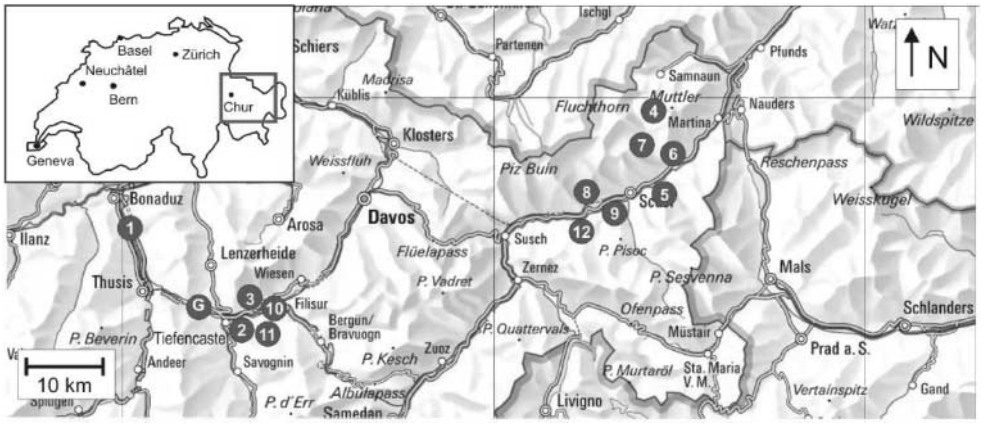

Figure 1. Location of studied mineralized springs in the Canton of Grisons, Switzerland, with sampling locations 1: Rothenbrunnen (Hinterrhein Valley), 2: Arvadi (Alvaneu Valley), 3: Zuepler (Alvaneu Valley), 4: Val Sinestra, 5: Lischana, 6: Rablönch, 7: Clozza, 8: Fuschna, 9: Carola (all Lower Engadine Valley), 10: Sulphur Spring, 11: Iron Spring (both Albula Valley), 12: Bonifacius (Lower Engadine Valley), G: Former gypsum mine at Alvaschein. © Reproduced with permission of swisstopo (BA 15039).
Source: http://map.geo.admin.ch/

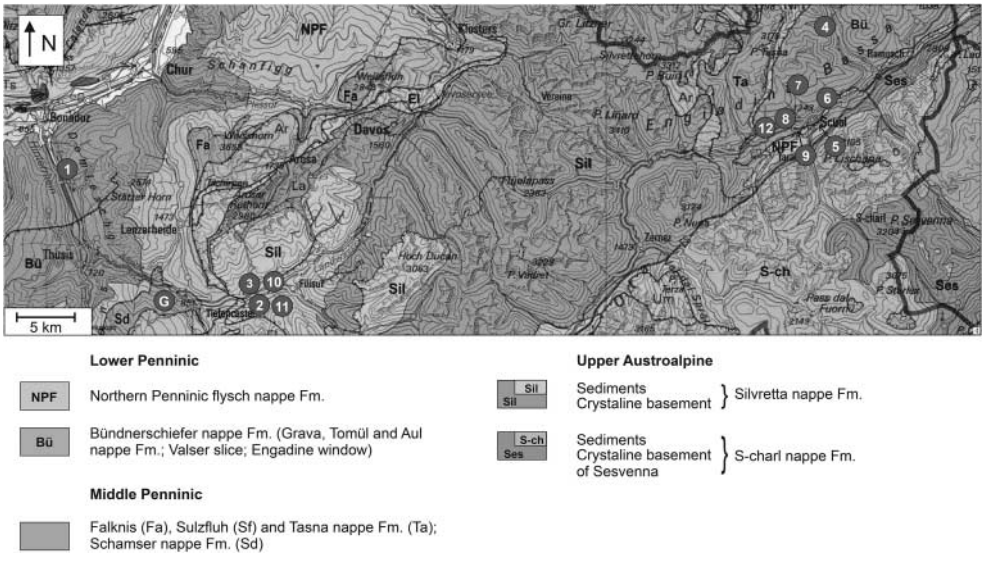

Figure 2. Regional geologic map of the study area; location of sampling sites as in Figure 1. © Reproduced with permission of swisstopo (BA 15039).
Source: http://map.geo.admin.ch/

to the Silvretta nappe in the NW and the S-charl-Sesvenna nappe in the SE, both of which have Mesozoic sedimentary cover rocks overlying crystalline basement. The springs discharge from the tectonically uncovered carbonaceous shales and marls of the Jurassic Bündner Schiefer, with the exception of the Lischana spring that is located in the Ramosch zone consisting of ophiolites and serpentinites of the middle Penninic nappes followed by granitic rocks of the Tasna nappe [33].

The springs in the Albula Valley are located in the crystalline rocks of the Silvretta nappe, which overlays carbonates and evaporitic gypsum, whereas the Rothenbrunnen spring discharges again from the Jurassic Bündner Schiefer.

3. Samples and analytical methods

Water samples were collected in the fall of 2009, 2011, and 2012 from 15 different mineralized springs in the Lower Engadin, Switzerland: near Scuol and Tarasp in the Inn Valley, near Alvaneu Bad about 20 km SW of Davos, and in Rothenbrunnen about 20 km SW of Chur (Table 1). Immediately after sample recovery, basic physico-chemical parameters (*T*, pH, electrical conductivity, and oxygen concentration) were determined using a WTW® multi 340i system.

Selected cations (Ca^{2+}, Mg^{2+}, Na^{+}, K^{+}, Sr^{2+}, Al^{3+}, and Fe^{2+}) were measured via ICP-OES (Spectro Flame EOP) from an acidified (5 drops of concentrated HNO_3 in 100 mL) aliquot, and selected anions (Cl^{-}, SO_4^{2-}, NO_2^{-}, NO_3^{-}, and PO_4^{3-}) were measured with ion chromatography (Methrom Compact IC761).

All spring water samples were analysed for hydrogen ($\delta^2H_{H_2O}$) and oxygen ($\delta^{18}O_{H_2O}$) isotopes at the stable isotope laboratory in Hannover. For hydrogen isotopes, 10 µL aliquots were measured with a fully automated chromium reduction system at 800 °C (H/Device, ThermoFinnigan) directly coupled to the dual inlet system of a Thermo Finnigan Delta XP isotope ratio mass spectrometer (IRMS). Oxygen isotopes were measured out of 0.5 mL sample aliquots with an automated equilibration unit (Gasbench II, ThermoFinnigan) interfaced with a continuous flow inlet to an IRMS. All samples were measured at least in duplicate and results are principally given in the standard delta notation as per mil relative to the VSMOW/VSLAP scale. External reproducibility (1σ) was better than 0.7 and 0.10 ‰ for δ^2H and $\delta^{18}O$, respectively.

For sulphate sulphur and oxygen isotope measurements, dissolved sulphate was first filtered (cellulose nitrate filter, 0.45 μm pore diameter) and subsequently precipitated as $BaSO_4$ at subboiling temperature (80 °C) at pH 2 using an 8.5 % $BaCl_2$ solution. Sulphur isotopic measurements ($\delta^{34}S$) were performed using a Carlo Erba Elemental Analyzer interfaced to a ThermoFinnigan Delta Plus (EA-IRMS). For this, approximately 200 µg of $BaSO_4$ precipitate was mixed with an equal amount of V_2O_5 and placed in a tin cup. Results are reported in the standard delta notation as per mil difference to the Canon Diablo Troilite (V-CDT). Reproducibility (1σ) as determined from replicate measurements was generally better than ± 0.3 ‰. Accuracy was monitored with internal lab standards and international reference materials (IAEA S1, S2, S3, and NBS 127). Oxygen isotopes were measured via high-temperature combustion (1450 °C) with a TC/EA coupled to a ThermoFinnigan Delta Plus XL. For this, approximately 200 µg of $BaSO_4$ precipitate was placed in a silver cup and combusted to carbon monoxide in a graphite-glassy carbon reactor. Results are reported as $\delta^{18}O$ versus V-SMOW. Reproducibility

Table 1. Sample locations.

Spring			
	Lucius	46°47′19.61″N	10°16′44.27″E
12	Bonifacius	46°46′56.28″N	10°14′59.95″E
9	Carola	46°47′19.55″N	10°16′38.03″E
8	Fuschna, oben	46°47′10.19″N	10°15′36.11″E
8	Fuschna, unten	46°47′10.19″N	10°15′36.11″E
7	Clozza	46°48′16.62″N	10°18′00.10″E
6	Rablönch	46°48′19.58″N	10°19′20.41″E
4	Val Sinestra	46°51′04.72″N	10°20′14.91″E
2	Arvadi	46°39′50.62″N	9°38′16.45″E
	Alvaneu Bad	46°40′05.90″N	9°38′58.19″E
3	Zuelper	46°39′50.62″N	9°38′16.45″E
10	Sulphur Spring	46°40′17.16″N	9°39′17.56″E
11	Iron Spring	46°40′11.57″N	9°40′01.39″E
5	Lischana	46°47′38.80″N	10°18′36.38″E
1	Rothenbrunnen	46°46′12.05″N	9°25′33.55″E

as determined from replicate measurements was generally better than ± 0.5 ‰. Accuracy was monitored with an internal barium sulphate lab standard and international reference materials (NBS 127, IAEA-SO 5, and IAEA-SO 6).

Dissolved sulphide from spring waters near Alvaneu Bad (Zuelper, Arvadi, Sulphur Spring) was stabilized during sampling as zinc sulphide following the addition of zinc acetate solution (3 %). In the laboratory at the Westfälische Wilhelms-Universität Münster, sulphur was liberated as hydrogen sulphide via reaction with 1 M chromous chloride solution following [34] and precipitated as silver sulphide (Ag_2S).

Elemental sulphur stored in the cells of *Thiothrix* bacteria collected at Arvadi and Zuelper was extracted with reagent-grade acetone. Subsequently, the acetone extract was filtered (0.45 µm) and reacted with 1 M chromous chloride solution (following [34]), and the resulting hydrogen sulphide was precipitated as silver sulphide.

Additional samples were obtained from elemental sulphur precipitates coating leaves and pebbles around Sulphur Spring near Alvaneu Bad. Whitish-yellow sulphur was carefully scraped off and also liberated via acetone extraction, followed by reaction with 1 M chromous chloride solution and final precipitation as silver sulphide.

For sulphur isotope analyses ($\delta^{34}S$), approximately 200 µg of Ag_2S was mixed with an equal amount of V_2O_5, placed in a tin cup, and measured via EA-IRMS with a Carlo Erba Elemental Analyser interfaced to a ThermoFinnigan Delta Plus IRMS. Results are reported in the standard delta notation as per mil difference to the Canon Diablo Troilite (V-CDT). Reproducibility (1σ) as determined from replicate measurements was generally better than ± 0.3 ‰. Accuracy was monitored with internal lab standards and international reference materials (IAEA S1, S2, S3, and NBS 127).

In addition to spring waters, Upper Triassic massive gypsum was collected at a small road cut close to the former gypsum mine at Alvaschein near Alvaneu Bad, and a Rauhwacke was sampled at Weissenstein, Albula Pass. Rock samples were pulverized, dissolved in a 10 % NaCl solution, and sulphate was re-precipitated as barium sulphate following the addition of a 8.5 % $BaCl_2$ solution. Furthermore, a sample of carbonaceous shale from the lower Jurassic Bündner Schiefer was collected at a road cut near Alvaneu Bad. Pyrite sulphur was liberated via chromous chloride reduction [27] and precipitated as silver sulphide. Again, sulphur isotope measurements of barium sulphate and silver sulphide precipitates were performed via EA-IRMS as described above.

Finally, occurrences of sulphide-oxidizing *Thiothrix* bacteria were sampled from Arvadi, Zuelper, and Sulphur Spring for sulphur isotope analyses.

For SEM analyses, small sample volumes of *Thiothrix* were collected in 2.5 ml Eppendorf tubes and fixed at the field site by adding an equal volume of 3 % glutaraldehyde solution to the aqueous samples. The fixative was pipetted off after approximately 6 h, and the samples were washed gently three times with source water. In order to prevent collapse of cells in the vacuum of the SEM, fixed samples were dehydrated in the laboratory by replacing the water stepwise with solutions containing 40, 60, 80, 90 and 100 % ethanol. Small amounts of dehydrated sample were placed on 13 mm white polycarbonate filters (Nuclepore, 0.2 µm pore size), the filters were placed on SEM stubs and remaining ethanol was replaced with pressurized liquid CO_2 for critical point drying. Dry specimens were contrasted by sputter coating with carbon (1–2 nm thickness). The procedure fixes samples well; in particular, it prevents the thin exopolymeric films from condensing into strand-like artefacts.

For SEM measurements, the electron beam (acceleration voltage between 2 and 5 kV) was focused on small spots where the cell density was not too dense. The images were taken by recording the intensity of backscattered and secondary electrons on a Zeiss Supra 50 VP field emission scanning electron microscope equipped with an in-lens secondary electron detector, a Centaurus backscattered electron detector and an EDX detector system.

For selected samples, multiple sulphur isotope measurements (^{32}S, ^{33}S, ^{34}S, and ^{36}S) were performed. Approximately 2 mg of silver sulphide precipitates from dissolved sulphide, dissolved sulphate (barium sulphate precipitates were first converted to silver sulphide via reaction with Thode solution [35]) and elemental sulphur (also previously converted to silver sulphide) were fluorinated to sulphur hexafluoride (SF_6) in nickel reactors (cf. [36]) at 300 °C with a fivefold excess of fluorine. Following cryogenic and gas chromatographic purification, the multiple sulphur isotope measurements were performed on a ThermoScientific MAT 253. Results are reported as $\delta^{34}S$, $\Delta^{33}S$ and $\Delta^{36}S$. $\Delta^{33}S$ values were calculated from $\delta^{33}S$ and $\delta^{34}S$ values (following [37,38]) as

$$\Delta^{33}S = \delta^{33}S - 1000 \times \left(\left(1 + \frac{\delta^{34}S}{1000}\right)^{0.515} - 1\right).$$

Reproducibility for $\Delta^{33}S$ (i.e. including fluorination) was better than ± 0.01 ‰ (1σ).
$\Delta^{36}S$ were calculated from $\delta^{36}S$ and $\delta^{34}S$ values (following [37,38]) as

$$\Delta^{36}S = \delta^{36}S - 1000 \times \left(\left(1 + \frac{\delta^{34}S}{1000}\right)^{1.90}\right) - 1,$$

and the reproducibility was better than ± 0.2 ‰ (1σ).

4. Results

All results are provided in subsequent tables and figures. We report $\Delta^{36}S$ data in order to expand the $\Delta^{36}S$ data set for meteoric water systems, but our interpretation regarding source identification and microbial sulphur cycling is based on $\delta^{34}S$ and $\Delta^{33}S$ only due to very limited nature of literature data so far.

4.1. *Spring waters*

Basic physico-chemical parameters (see Table 2) were highly variable among the different springs with pH ranging from 5.9 to 6.5 in the Scuol-Tarasp area and from 7.2 to 7.9 for springs near Alvaneu Bad. Temperatures varied between 7.8 and 18.5 °C with no regional trend discernible. Dissolved oxygen concentrations varied between 0.1 and 11.0 mg L^{-1}, again with no clear distinction between the sampling areas. Finally, electrical conductivity displayed a range between 1220 and 8400 µS cm^{-1}, again with no regional distinction discernible.

Cation and anion concentrations are equally variable (see Table 2). Wexsteen et al. [1] and Bissig [2] grouped the mineralized springs of the Lower Engadin depending upon their ionic species and location. Accordingly, the springs Bonifacius, Carola and Fuschna are characterized as Ca–Na–HCO_3–SO_4 waters and form one group of springs that are located in the Inn Valley (here called Group 1 springs). Val Sinestra, Rablönch and Clozza discharge Ca–HCO_3 waters along the slope near Scuol (here called Group 2 springs). Mineralized springs of Group 3 are located near Alvaneu Bad (Arvadi, Alvaneu Bad, Zuelper, Sulphur Spring, Iron Spring) and discharge Ca–Na–HCO_3–Cl–SO_4 water. The springs at Lischana and Rothenbrunn form a fourth group which is characterized by their Na, Mg, HCO_3, and SO_4 content.

Hydrogen and oxygen isotopes of spring water samples varied between -114.9 and -91.1 ‰ for hydrogen ($\delta^2H_{H_2O}$) and between -15.4 and -11.5 ‰ for oxygen ($\delta^{18}O_{H_2O}$) isotopes, respectively (Table 3).

Table 2. Basic parameters, cation and anion data for the different sampling campaigns.

No.[a]	Spring	T (°C)	pH	Conductivity (µS cm^{-1})	O_2	Ca^{2+}	Mg^{2+}	Sr^{2+}	Na^{+}	K^{+}	Al^{3+} (mg L^{-1})	Fe^{2+}	Cl^{-}	SO_4^{2-}	NO_2^{-}	NO_3^{-}	PO_4^{3-}
2009 sampling campaign																	
	Na–HCO_3–Cl water																
	Lucius												2452	1779	bdl	22.41	bdl
	Ca–Na–HCO_3–SO_4 water (Group 1)[b]																
12	Bonifacius												21	175	bdl	bdl	bdl
9	Carola												318	468	bdl	1.69	bdl
8	Fuschna, oben												9.2	83	bdl	bdl	bdl
8	Fuschna, unten												7.1	88	bdl	bdl	bdl
	Ca–HCO_3 water (Group 2)[b]																
7	Clozza												2.6	84	bdl	bdl	bdl
6	Rablönch																
4	Val Sinestra																
	Ca–Na–HCO_3–Cl–SO_4 water (Group 3)[b]																
2	Arvadi												11.2	908	bdl	23.76	bdl
	Alvaneu Bad																
3	Zuelper												3.2	1210	bdl	1.14	bdl
10	Sulphur Spring																
11	Iron Spring																
	Na–Mg–HCO_3–SO_4 water (Group 4)[b]																
5	Lischana												170	1673	bdl	bdl	bdl
1	Rothenbrunn												10.8	90	bdl	bdl	bdl
2011 sampling campaign																	
	Na–HCO_3–Cl water																
	Lucius																
	Ca–Na–HCO_3–SO_4 water (Group 1)[b]																
12	Bonifacius	8.0	6.38	4900	0.51	923	120	13.1	608	26.8	bdl	3.56	na	182	nd	nd	nd
9	Carola	10.3	6.07	3730	1.83	523	98.2	5.08	463	22.1	bdl	0.44	363	542	bdl	bdl	nd
8	Fuschna, oben																
8	Fuschna, unten	11.7	6.20	3480	0.73	904	89.0	5.38	140	12.1	0.03	2.73	2.63	94.0	bdl	bdl	nd
	Ca–HCO_3 water (Group 2)[b]																
7	Clozza	8.5	5.90	1690	0.10	423	45.5	2.13	3.23	1.07	bdl	3.49	bdl	87.2	bdl	bdl	nd
6	Rablönch	14.5	7.71	1940	8.02	493	47.0	3.08	62.4	4.31	0.08	6.62	47.9	69.9	bdl	bdl	nd
4	Val Sinestra	9.3	6.25	3920	2.70	429	75.3	4.58	569	31.4	bdl	8.22	433	214	0.58	bdl	nd

(*Continued*).

Table 2. Continued.

	Ca–Na–HCO_3–Cl–SO_4 water (Group 3)[b]																
2	Arvadi	8.9	7.85	1630	9.80	331	92.9	21.6	1.94	1.20	bdl	0.15	bdl	961	bdl	0.38	nd
	Alvaneu Bad																
3	Zuelper	13.2	7.20	1950	3.19	408	131	16.7	2.26	1.12	bdl	bdl	bdl	1287	bdl	0.07	nd
10	Sulphur Spring	12.1	7.40	1220	0.90	246	77.7	4.57	2.58	0.91	bdl	bdl	1.37	654	bdl	bdl	nd
11	Iron Spring	10.8	7.27	2140	0.09	468	142	13.8	2.45	0.82	bdl	0.30	0.96	1372	bdl	4.52	nd
	Na–Mg–HCO_3–SO_4 water (Group 4)[b]																
5	Lischana	9.1	6.39	6080	0.69	236	412	5.09	1150	44.1	bdl	0.05	113	1086	bdl	bdl	nd
1	Rothenbrunn	18.5	6.52	1600	0.48	171	50.2	2.67	95.6	4.38	bdl	2.45	6.22	99.0	bdl	bdl	nd
2012 sampling campaign																	
	Na–HCO_3–Cl water																
	Lucius																
	Ca–Na–HCO_3–SO_4 water (Group 1)[b]																
12	Bonifacius	6.39	8.1	4990	1.28	853	105	11.2	536	27.7	0.05	7.38	bdl	223	bdl	bdl	23.2
9	Carola	6.03	8.8	3330	2.70	466	85.8	4.31	303	13.4	0.01	0.36	bdl	552	bdl	bdl	26.5
8	Fuschna, oben																
8	Fuschna, unten	6.34	10.1	3550	0.52	850	82.4	5.24	125	11.2	0.03	2.73	2.87	105	bdl	bdl	16.3
	Ca–Na–HCO_3–Cl–SO_4 water (Group 3)[b]																
7	Clozza	5.94	12.4	1740	0.44	425	49.6	2.00	6.82	1.19	0.02	3.25	0.01	103	bdl	bdl	14.8
6	Rablönch	6.13	11.5	2140	1.69	471	47.5	2.79	54.9	3.97	0.09	6.03	0.64	63.3	bdl	bdl	31.5
4	Val Sinestra	6.30	11.4	4020	1.47	399	70.4	4.08	525	29.9	0.07	8.53	0.20	237	bdl	bdl	15.8
	Ca–Na–HCO_3–Cl–SO_4 water (Group 3)[b]																
2	Arvadi	7.88	7.8	1653	11.00	338	97.2	22.1	4.25	1.31	0.02	0.02	1.60	1022	0.12	0.49	2.02
	Alvaneu Bad																
3	Zuelper	7.36	12.1	1982	3.42	406	130	17.7	4.99	1.21	0.02	0.02	2.06	1377	2.26	0.26	2.15
10	Sulphur Spring					242	77.2	4.67	4.44	0.95	0.57	0.71	0.88	733	bdl	bdl	1.04
11	Iron Spring	7.30	8.4	2150	1.35	459	135	14.7	5.98	0.91	0.02	0.27	1.55	1641	bdl	0.43	0.78
	Na–Mg–HCO_3–SO_4 water (Group 4)[b]																
5	Lischana	6.53	9.6	8400	0.82	294	525	6.38	1441	56.8	bdl	0.03	0.15	1528	bdl	bdl	30.3
1	Rothenbrunn																

Note: bdl, below detection limit; nd, not determined.
[a]No. refers to numbers in Figures 1 and 2.
[b]Water classification according to [1–3].

Table 3. Hydrogen and oxygen isotopes of spring waters.

No.[a]	Spring	Water type[b]	δ^2H	δ^{18}O
			‰ V-SMOW	
	Lucius	Na–HCO_3–Cl	− 93.6	− 11.51
12	Bonifacius	Ca–Na–HCO_3	− 114.9	− 15.38
9	Carola	Ca–HCO_3–SO_4	− 98.6	− 13.00
8	Fuschna, oben	Ca–HCO_3	− 112.7	− 14.85
8	Fuschna, unten	Ca–HCO_3	− 112.2	− 14.75
7	Clozza	Ca–HCO_3	− 106.5	− 14.28
2	Arvadi		− 91.1	− 12.32
3	Zuelper		− 93.6	− 12.74
5	Lischana	Na–Mg–HCO_3–SO_4	− 105.7	− 14.10
1	Rothenbrunn		− 91.6	− 12.64

[a]No refers to numbers in Figures 1 and 2.
[b]Water type according to [2].

Dissolved sulphate from the mineralized springs (Table 4) displayed sulphur isotopes ($\delta^{34}S_{SO_4}$) ranging from − 9.2 to + 20.6 ‰. The sulphate oxygen isotopic composition ($\delta^{18}O_{SO_4}$) varied between − 3.3 and + 18.3 ‰. Δ^{33}S and Δ^{36}S values for sulphate varied between − 0.037 and 0.000 ‰, and between 0.353 and 0.557 ‰, respectively.

Dissolved sulphide (Table 5) of the Zuelper spring showed δ^{34}S, Δ^{33}S, and Δ^{36}S values of − 25.1, 0.006, and 0.204 ‰, respectively, whereas sulphide from Sulphur Spring was characterized by a δ^{34}S value of − 21.5 ‰ and Δ^{33}S and Δ^{36}S values of 0.064 and 0.031 ‰, respectively.

4.2. *Elemental sulphur from Thiothrix bacteria and sulphur precipitates*

Sulphur isotope values for elemental sulphur (Table 5) were generally negative. Granular elemental sulphur contained within the filaments of *Thiothrix* bacteria collected at Arvadi and Zuelper displayed δ^{34}S values between − 26 and − 23 ‰, Δ^{33}S values between 0.025 and 0.041 ‰, and Δ^{36}S values between 0.362 and 0.519 ‰. Thin whitish films of elemental sulphur covering pebbles and dead leaves in the discharge area of Sulphur Spring exhibited δ^{34}S values between − 28 and − 26 ‰, a Δ^{33}S value of 0.064 ‰, and Δ^{36}S value of 0.093 ‰.

4.3. *Rock samples*

The Upper Triassic gypsum samples displayed sulphur and oxygen isotope values of 15.1 ‰ and between 17.9 and 19.9 ‰, respectively. Pyrite sulphur from the Lower Jurassic Bündner Schiefer showed a δ^{34}S value of − 15.6 ‰.

5. Discussion

5.1. *Unravelling the source of dissolved sulphate*

In principle, dissolved sulphate in ground and spring water can have multiple sources, including the dissolution of evaporites and/or the oxidation of sulphide minerals, both indicating water–rock interaction in the subsurface. In addition, an atmospheric contribution of sulphate via precipitation that percolates through the soil into the groundwater is also possible. This latter source of dissolved sulphate might include an anthropogenic contribution of sulphate. Because

Table 4. Sulphur and oxygen isotopes of spring water sulphate.

		2009		2011			2012		
No.[a]	Spring	SO_4 (mg L^{-1})	$\delta^{34}S$ (‰) V-CDT	SO_4 (mg L^{-1})	$\delta^{34}S$ (‰) V-CDT	$\delta^{18}O$ (‰) V-SMOW	SO_4 (mg L^{-1})	$\delta^{34}S$ (‰) V-CDT	$\delta^{18}O$ (‰) V-SMOW
	Na–HCO_3–Cl water								
	Lucius	1779	17.6						
	Ca–Na–HCO_3–SO_4 water (Group 1)[b]								
12	Bonifacius	175	19.1		19.0	13.2	223	19.1	12.7
9	Carola	468	11.9	542	12.3	11.1	552	11.3	10.0
8	Fuschna, oben	83	–0.9						
8	Fuschna, unten	88	–3.3	94	–2.8	1.9	105	–3.1	1.9
	Ca–HCO_3 water (Group 2)[b]								
7	Clozza	84	–9.1	87	–8.6	–2.6	104	–9.2	–3.3
6	Rablönch			70	–8.2	0.7	63	–8.7	0.6
4	Val Sinestra			214	8.9	10.4	237	9.0	9.7
	Ca–Na–HCO_3–Cl–SO_4 water (Group 3)[b]								
2	Arvadi	908	15.5	961	15.3	15.8	1022	15.4	15.8
	Alvaneu Bad			99	20.3	10.6			
3	Zuelper	1210	17.7	1286	17.4	17.7	1377	17.4	16.3
10	Sulphur Spring			654	20.2	15.5	733	20.6	14.4
11	Iron Spring			1372	18.2	18.3	1641	18.4	16.6
	Na–Mg–HCO_3–SO_4 water (Group 4)[b]								
5	Lischana	1673	18.1	1086	17.6	12.4	1528	17.8	13.3
1	Rothenbrunn	53	2.9	99	3.0	6.6			

[a]No refers to numbers in Figures 1 and 2.
[b]Water classification according to [1–3].

Table 5. Multiple sulphur isotopes of dissolved sulphur species for selected springs.

		Sulphate			Sulphide			Elemental sulphur		
No.[a]	Spring	δ^{34}S (‰) V-CDT	Δ^{33}S (‰)	Δ^{36}S (‰)	δ^{34}S (‰) V-CDT	Δ^{33}S (‰)	Δ^{36}S (‰)	δ^{34}S (‰) V-CDT	Δ^{33}S (‰)	Δ^{36}S (‰)
2	Arvadi 2011	15.3								
2	Arvadi 2011 *Thiothrix*							− 25.6		
2	Arvadi 2011 *Thiothrix*							− 24.1		
3	Zuelper 2011	17.4								
3	Zuelper 2011 *Thiothrix*							− 23.8		
3	Zuelper 2011 *Thiothrix*							− 22.9		
10	Sulphur Spring 2011	20.2								
10	Sulphur Spring 2011 pebbles							− 27.0		
10	Sulphur Spring 2011 leaves							− 26.8		
2	Arvadi 2012	15.5	− 0.009	0.557						
2	Arvadi 2012 *Thiothrix*							− 26.0	0.041	0.519
3	Zuelper 2012	18.0	0.000	0.497	− 21.5	0.006	0.204			
3	Zuelper 2012 *Thiothrix*							− 24.2	0.025	0.362
10	Sulphur Spring 2012	21.3	− 0.007	0.521	− 25.1	0.064	0.031			
10	Sulphur Spring 2012 pebbles							− 27.5	0.064	0.093
7	Clozza 2012	− 9.7	− 0.037	0.353						

[a]No. refers to numbers in Figures 1 and 2.

each of these sources has different sulphur and oxygen isotopic compositions, variable sulphur and oxygen isotope results can be expected for the different spring water samples.

Based on the mineralization observable in the spring waters, Bissig et al. [3] developed a conceptual model for their origin. These authors propose the deep subsurface circulation of meteoric water and associated water–rock interaction and the mixing with shallow subsurface water. Water discharging at the mineralized springs of the Lower Engadine displays hydrogen and oxygen isotope values that broadly resemble the isotopic composition of regional meteoric water as sampled in precipitation and river water (Figure 3). The range in δ^2H and δ^{18}O for spring waters is substantially reduced compared to the local precipitation collected at Pontresina but not as narrow as water from the Inn river (Source of data: Swiss Bundesamt für Umwelt BAFU and Nationale Grundwasserbeobachtung NAQUA). Spring waters define a regression line that is comparable to the local meteoric water line as defined by the local precipitation and the regional river water.

The sulphate concentration is relatively constant for every spring when comparing the individual sampling campaigns (Figure 4) due to the fact that sampling occurred approximately at the same time each year (August to September). Minor differences result from dilution/concentration effects depending on the prevailing water balance. In contrast, sulphate concentrations are distinctly different between individual springs with low values below 100 mg L^{-1} and high values above 1500 mg L^{-1}. Moreover, each spring exhibits a unique sulphur isotopic composition within a total range in δ^{34}S between -9.1 and $+20.6$ ‰. In addition, a correlation between sulphate concentration and sulphur isotopic composition is clearly discernible (Figure 4). Springs that have a high sulphate concentration are also characterized by positive δ^{34}S values, whereas those with a low sulphate concentration display less positive or even negative δ^{34}S values. Bonifacius spring, however, represents an exception to this correlation as it is discharging water with a low sulphate concentration, but the sulphate exhibits a positive δ^{34}S value around $+19$ ‰. In

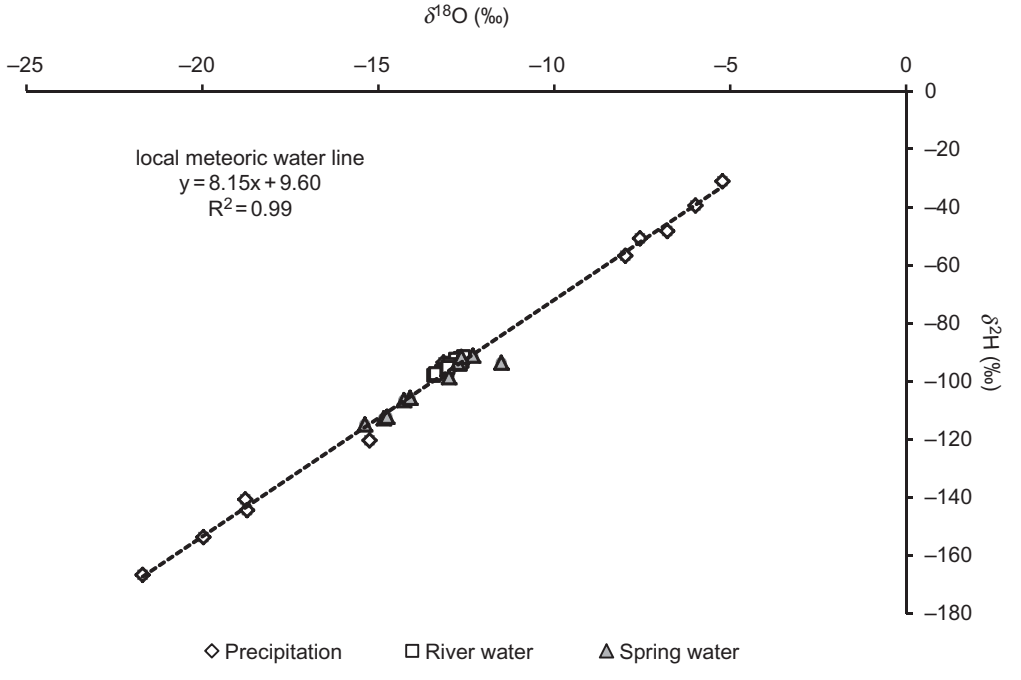

Figure 3. Hydrogen and oxygen isotopes for spring waters compared to regional precipitation and Inn river water. Local meteoric water line based on precipitation data.

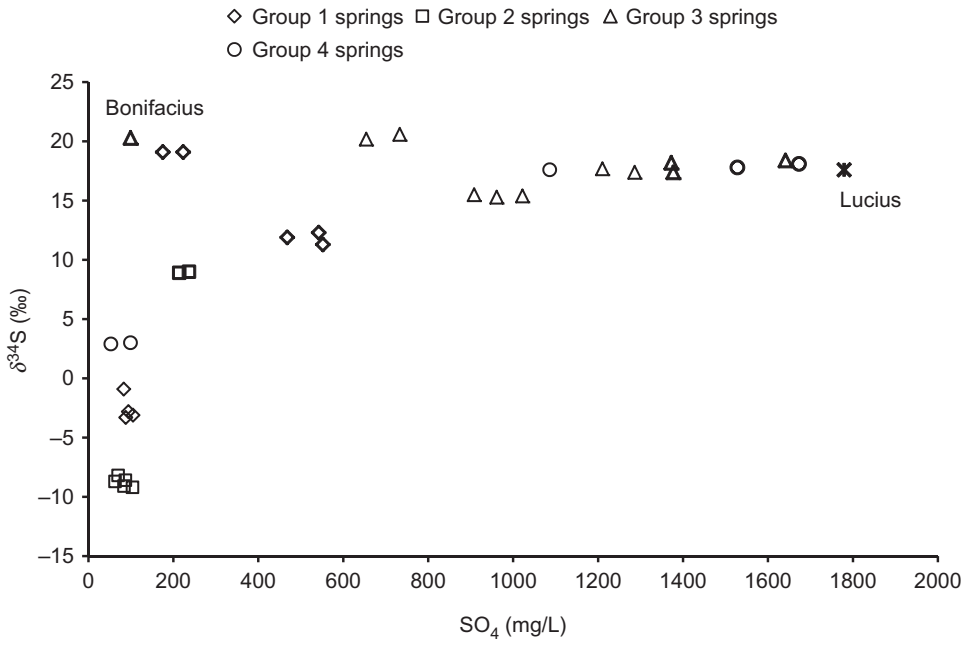

Figure 4. Sulphate concentration and $\delta^{34}S$ values of spring water sulphate (grouping of springs according to [2,3]).

addition to the relationship between sulphate concentration and sulphate sulphur isotopic composition, a clearly positive correlation exists between the $\delta^{34}S_{SO4}$ and $\delta^{18}O_{SO4}$ values for these spring waters (Figure 5). Both correlations, that is, between sulphate concentration and both sulphate isotopes suggest that the individual springs derive their sulphate from different sources. Considering the deep circulation pattern suggested in [3] for the springs of the Lower Engadine, the distinctly different sulphate concentrations and their sulphur and oxygen isotopic compositions indicate water–rock interaction in the subsurface, involving quite different rock types (Figure 5).

In general, springs that discharge water with a high sulphate concentration (such as the Group 3 springs Arvadi, Zuelper, Sulphur Spring, and Iron Spring in the Albula Valley) with sulphate concentrations partly well above 600 mg L^{-1} are located in the sedimentary cover rocks of the Silvretta nappe that comprise carbonate and evaporites. The Triassic aged gypsum occurrence near the town of Alvaschein and the Rauhwacke from Weissenstein (Albula Pass) and their sulphur and oxygen isotope values around $+15$ ‰ and between $+18$ and $+20$ ‰, respectively, would be consistent with the interpretation that evaporite dissolution represents the source for the sulphate of the Group 3 springs, given their isotopic compositions between $+15$ and $+23$ ‰ ($\delta^{34}S_{SO4}$) and between $+10$ and $+20$ ‰ ($\delta^{18}O_{SO_4}$), respectively. In addition to the high sulphate concentrations and sulphur and oxygen isotopic compositions, high concentrations of strontium in the Arvadi, Zuelper and Iron springs are also consistent with the subsurface dissolution of evaporites.

Comparably heavy sulphur and oxygen isotopic compositions were measured for dissolved sulphate at the Lischana and Bonifacius springs, although spring water at Bonifacius (Group 1 spring) shows considerably lower sulphate concentrations (around 200 mg L^{-1}) compared to Lischana (>1000 mg L^{-1}). Both springs are located in stratigraphic units that do not contain evaporitic rocks. Bonifacius spring discharges from the Jurassic Bündner Schiefer. However, based on hydrogen and oxygen isotopes, Wexsteen et al. [1] argued that the recharge area for

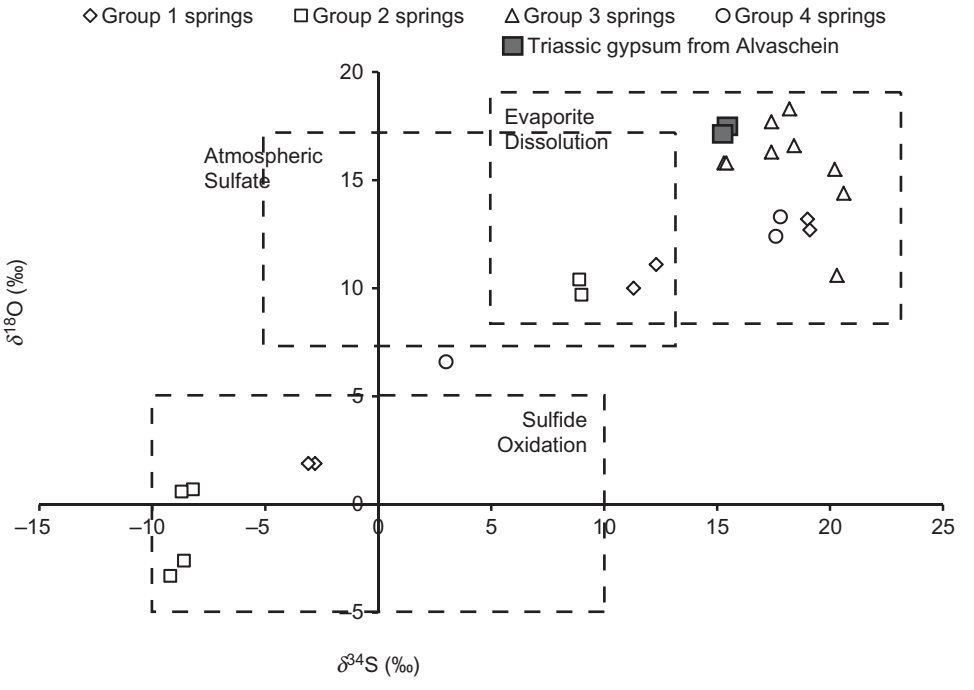

Figure 5. $\delta^{34}S$ and $\delta^{18}O$ values of spring water sulphate (grouping of springs according to [2,3]; sulphate source identification according to [4]).

the Bonifacius spring was located in an altitude of 2470 ± 70 m, and that the interaction with carbonate rocks north of the Engadine Window would be a possible source for the sulphate of this spring. The Lischana spring, in contrast, discharges from ophiolites and serpentinites in the Ramosch zone. High magnesium and sodium concentrations in the spring water suggest intense water–rock interaction with silicate rocks in the subsurface. Following Wexsteen et al. [1], the sulphate could be derived from meteoric dissolution of evaporites of the Tasna nappe, but evaporitic rocks are also present in the S-charl-Sesvenna nappe. A sulphate concentration of around 500 mg L^{-1}, a $\delta^{34}S$ value of $+12$ ‰ and a $\delta^{18}O$ value of $+11.5$ ‰ suggest that the dissolution of evaporites is at least partly responsible for the sulphate load of the Carola spring water. Bissig et al. [3] classified the Carola spring water as a mixture between deeply circulating water that interacts with the crystalline basement rocks and shallower sulphate-rich groundwater from a regional aquifer. In particular, the lower sulphur and oxygen isotope values that were measured for the Carola sulphate indicate that evaporite dissolution is not the sole source of dissolved sulphate. An atmospheric contribution of sulphate can be largely excluded as both sulphate concentration and isotopic composition would not match the characteristics of the spring water. Thus, a contribution from the microbial oxidation of sulphide sulphur in the deeper subsurface is indicated. Geographically closely located is the Rablönch spring with a water low in sulphate and exhibiting a negative sulphate sulphur isotopic composition around -8 ‰ and a low sulphate oxygen isotopic composition around 0 ‰. All of this would be consistent with microbial sulphide oxidation as an additional source for some of the dissolved sulphate load.

Group 2 springs, Fuschna spring and Rothenbrunnen spring all show low sulphate concentrations (all but Fuschna below 100 mg L^{-1}) and sulphur and oxygen isotope values that are substantially less positive (or even negative) than measured for the Group 3 springs. In fact, sulphate in these spring waters displays $\delta^{34}S$ values between -15 and $+4$ ‰ and $\delta^{18}O$ values between -5 and $+5$ ‰, values that are suggestive of sulphide oxidation (cf. [4]). It should be

noted that pyrite from the Jurassic Bündner Schiefer collected in the area showed a low $\delta^{34}S$ value of -15.6 ‰, comparable to a generally negative sulphur isotopic composition of sedimentary sulphide (e.g. [14,39]). Subsurface oxidative weathering of sedimentary pyrite would release sulphate with an equally negative $\delta^{34}S$ value, as little to no sulphur isotopic fractionation is associated with sulphide oxidation (e.g. [28]). The oxygen isotopic composition of sulphate derived via sulphide oxidation can be variable depending on the isotopic composition of the oxygen involved [5,7,21]. Sulphate derived from pyrite oxidation involving oxygen that was largely (or entirely) derived from the water molecule would exhibit a clearly negative $\delta^{18}O$ value. Interestingly, water from Group 2 springs, Fuschna and Rothenbrunnen, exhibits high concentrations of dissolved iron which would be consistent with the dissolution of pyrite but also with anoxic groundwater conditions. Upon discharge, the dissolved Fe^{2+} would be oxidized to Fe^{3+} and precipitate as iron(III)oxyhydroxide as can be observed at Clozza and Rothenbrunnen. Independent evidence suggests a contribution from microbial iron oxidation [40] for this redox reaction.

An atmospheric contribution of sulphate from precipitation cannot be ruled out in principle, but the sulphate concentrations of all springs studied here are distinctly higher than the sulphate concentration of central European precipitation (e.g. 1 mg L^{-1} for northern Italy, cf. [41]). Similarly, the $\delta^{34}S$ and $\delta^{18}O$ values recorded for atmospheric sulphate range from 0 to $+5$ ‰ and $+8$ to $+15$ ‰, respectively[4], which is outside the isotopic compositions measured here for spring water samples. Both observations, that is, a low sulphate concentration and decidedly different sulphate sulphur and oxygen isotopic compositions rule out a substantial atmospheric contribution, let alone the only source of spring water sulphate.

In summary, variable sulphate concentrations but more so paired measurements of sulphur and oxygen isotopes from the dissolved sulphate load of springs from the Lower Engadin, Switzerland, indicate intense water–rock interaction in the subsurface as the principal source of that sulphate. This includes the dissolution of evaporites and the oxidation of pyrite in sediments and volcanic rocks as the two principle end members.

5.2. *Microbial sulphur cycling*

Microbiological evidence for intense and diverse microbial activities exists at several of the studied spring locations (Hanselmann, unpublished). With respect to microbial sulphur cycling, thick aggregates of white filamentous *Thiothrix* bacteria have been identified microscopically and via 16S rRNA gene sequencing (results available through the NCBI database at http://www.ncbi.nlm.nih.gov/nuccore/AB473985.1) at Arvadi and Zuelper (Figure 6). In addition, microbial sulphur cycling is known to be associated with the fractionation of sulphur (and oxygen) isotopes (e.g. [15,23,27,42,43]). In particular the springs near Alvaneu Bad and their sulphur and oxygen isotopic compositions are suggestive of intense and complex sulphur cycling that is, at least in part, microbially catalyzed.

Dissolved sulphide in the springs at Zuelper and Sulphur Spring displayed $\delta^{34}S$ values of -25.1 and -21.5 ‰, respectively, suggesting bacterial sulphate reduction as likely source for the dissolved sulphide. Positive $\delta^{34}S$ and $\delta^{18}O$ values for the dissolved sulphate in these two springs suggest the dissolution of evaporites as the likely source of dissolved sulphate in these springs. However, compared to the isotopic composition of the Triassic gypsum from the nearby Alvaschein locality, at least the sulphur isotopic composition of the dissolved sulphate at Zuelper and Sulphur Spring is somewhat enriched in ^{34}S. This observation would be consistent with sulphate reduction in the water that discharges at both springs. The apparent fractionation between dissolved sulphate and sulphide ($\delta^{34}S_{SO_4} - \delta^{34}S_{H_2S}$) varies between 39 ‰ (Zuelper) and 46 ‰ (Sulphur Spring) which is consistent with the process of bacterial sulphate reduction (e.g. [15]).

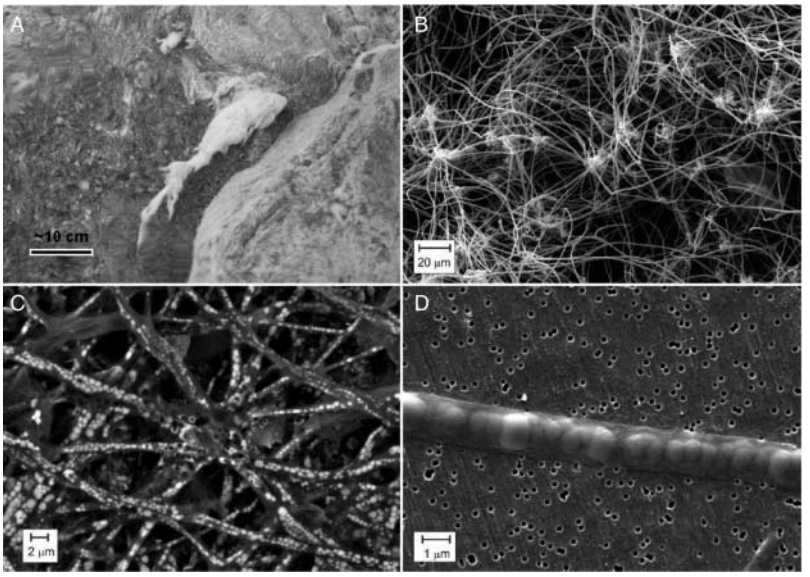

Figure 6. *Thiothrix* bacteria at Sulphur Spring. *Thiothrix* spp. are sessile filamentous 'sulfur bacteria'. They thrive naturally in masses in the hydrogen sulphide-rich outflow waters of sulphur springs where they form dense floating tufts that adhere to almost any surface (a); tufts consist of trichome assemblages that form rosette-like structures, so–called holdfasts which form the adhering 'glue' for the base cell of each trichome (b). The trichomes contain individual rod-shaped cells that are held together by extracellular sheaths (d). The most conspicuous cell inclusions are the large, white-appearing sulphur globules (c and d) (b–d are SEM images).

The Arvadi and Zuelper springs are characterized by sometimes abundant occurrences of white filamentous *Thiothrix* bacteria that store elemental sulphur in their cells. This elemental sulphur displayed also a ^{34}S depleted sulphur isotopic composition with $\delta^{34}S$ values ranging from -26 to -23 ‰ which is comparable (or slightly ^{34}S depleted) to the $\delta^{34}S$ values measured for dissolved sulphide. This strongly suggests that dissolved sulphide generated via microbial sulphate reduction under anoxic conditions in the subsurface was subsequently oxidized by sulphide-oxidizing bacteria, for example, *Thiothrix*, at the anoxic–oxic transition within the discharge area of the springs. Only a minor isotope effect is associated with microbial sulphide oxidation [28] as revealed here by the similarity in $\delta^{34}S$ of sulphide sulphur and elemental sulphur. Sulphide oxidation is also the likely source of elemental sulphur covering pebbles and dead leaves in the discharge pool of Sulphur Spring with $\delta^{34}S$ values at -27 ‰.

In addition to $\delta^{34}S$, the minor sulphur isotopes ^{33}S and ^{36}S were measured for a few samples of dissolved sulphate and sulphide as well as for elemental sulphur from the *Thiothrix* filaments from the Zuelper and Arvadi springs and from the thin film covering pebbles at Sulphur Spring. Following [29], the isotopic difference in ^{34}S and in ^{33}S between dissolved sulphate and dissolved sulphide and between sulphate and elemental sulphur points to bacterial sulphate reduction, whereas the isotopic differences (^{34}S and ^{33}S) between dissolved sulphide and elemental sulphur are consistent with microbial sulphide oxidation (Figure 7). A minor difference exists in $\Delta^{33}S$ between elemental sulphur stored in the cells of *Thiothrix* bacteria (0.025 and 0.041 ‰) and the elemental sulphur covering pebbles and leaves at Sulphur Spring (0.064 ‰). This could be indicative of a difference between microbial and inorganic sulphide oxidation, but more data would be necessary to clarify this possibility. In summary, multiple sulphur and oxygen isotopes of dissolved sulphate, dissolved sulphide and elemental sulphur indeed reveal intense microbial turnover of sulphur, specifically bacterial sulphate reduction and sulphide oxidation.

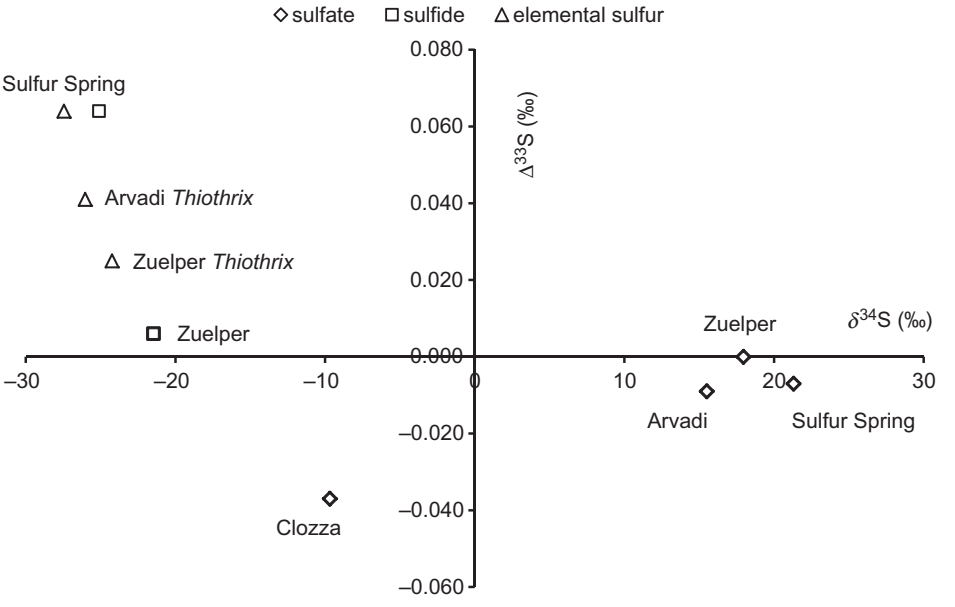

Figure 7. $\delta^{34}S$ and $\Delta^{33}S$ values for dissolved sulphate, sulphide, and elemental sulphur from selected springs in the Lower Engadine Valley, Switzerland.

6. Conclusions

Highly mineralized springs in the Scuol-Tarasp area of the Lower Engadine and near Alvaneu, Albula Valley, Switzerland, display distinct differences with respect to the source and fate of their dissolved sulphur loads. Dissolution of evaporites in the subsurface is causing high concentrations and associated positive sulphur and oxygen isotopes of the dissolved sulphate in selected springs. Supporting evidence stems from the sulphur and oxygen isotopic composition of Triassic calcium sulphate. In contrast, low sulphate concentrations and less positive or even negative $\delta^{34}S$ and $\delta^{18}O$ values indicate a substantial contribution of sulphate sulphur from the oxidation of sulphides in the crystalline basement rocks or the Jurassic sedimentary cover rocks. An anthropogenic sulphate contribution cannot be ruled out in principle but seems unreasonable considering the low sulphate concentration and isotopic composition of central European precipitation. Microbial sulphur cycling is clearly discernible through the multiple sulphur isotope signatures ($\delta^{34}S$, $\Delta^{33}S$) of dissolved sulphate and sulphide as well as of elemental sulphur stored in the cells of sulphide-oxidizing bacteria (*Thiothrix*) or covering surfaces in the immediate discharge area of sulphur rich springs. Microbial sulphate reduction and sulphide oxidation in the subsurface could be identified.

Acknowledgements

Samples for this study were collected during student field courses jointly held between the universities of Münster, Tübingen, Zürich, Basel, and Vienna in 2009, 2011, and 2012. Stimulating discussions with R. Schönberg, M. Obst, M. Lehmann, S. Krämer, and T. Eglinton are gratefully acknowledged. We thank the students from these universities for their help during sampling and initial measurements in the field and A. Reschka for ICP-OES and IC measurements in Münster. Maps in figures 1 and 2 are reproduced with permission of swisstopo (BA15039). The Swiss Bundesamt für Umwelt BAFU and the Nationale Grundwasserbeobachtung NAQUA are gratefully acknowledged for providing isotope data of river water and precipitation.

Disclosure statement

No potential conflict of interest was reported by the authors.

References

[1] Wexsteen P, Jaffe FC, Mazor E. Geochemistry of cold CO_2-rich springs of the Scuol-Tarasp region, Lower Engadine, Swiss Alps. J Hydrol. 1988;104:77–92.
[2] Bissig P. Die CO2-reichen Mineralquellen von Scuol-Tarasp (Unterengadin, Kt. GR). Bull Angew Geol. 2004;9: 39–47.
[3] Bissig P, Goldscheider N, Mayoraz J, Surbeck H, Vuataz F-D. Carbogaseous spring waters, coldwater geysers and dry CO_2 exhalations in the tectonic window of the Lower Engadine Valley, Switzerland. Eclogae Geol Helv. 2006;99:143–155.
[4] Clark I, Fritz P. Environmental isotopes in hydrogeology. London: CRC Press LLC; 1997.
[5] Calmels D, Gaillardet J, Brenot A, France-Lanord C. Sustained sulfide oxidation by physical erosion processes in the Mackenzie River basin: climatic perspectives. Geol. 2007;35:1003–1006.
[6] Tuttle MLW, Breit GN, Cozzarelli IM. Processes affecting δ^{34}S and δ^{18}O values of dissolved sulfate in alluvium along the Canadian River, central Oklahoma, USA. Chem Geol. 2009;265:455–467.
[7] Turchyn AV, Brüchert V, Lyons TW, Engel GS, Balci N, Schrag DP, Brunner B. Kinetic oxygen isotope effects during dissimilatory sulfate reduction: a combined theoretical and experimental approach. Geochim Cosmochim Acta. 2010;74:2011–2024.
[8] Yuan F, Mayer B. Chemical and isotopic evaluation of sulfur sources and cycling in the Pecos River, New Mexico, USA. Chem Geol. 2012;291:13–22.
[9] Hosono T, Lorphensriand O, Onodera S, Okawa H, Nakano T, Yamanaka T, Tsujimura M, Taniguchi M. Different isotopic evolutionary trends of δ^{34}S and δ^{18}O compositions of dissolved sulfate in an anaerobic deltaic aquifer system. Appl Geochem. 2014;46:30–42.
[10] Claypool GE, Holser WT, Kaplan IR, Sakai H, Zak I. The age curves of sulfur and oxygen isotopes in marine sulfate and their mutual interpretation. Chem Geol. 1980;28:190–260.
[11] Kampschulte A, Strauss H. The sulfur isotopic evolution of Phanerozoic seawater based on the analysis of structurally substituted sulfate in carbonates. Chem Geol. 2004;204:255–286.
[12] Strauss H. 4 Ga of seawater evolution: evidence from the sulfur isotopic composition of sulfate. Geol Soc Am Spec Pap. 2004;379:195–205.
[13] Longinelli A. Oxygen-18 and sulphur-34 in dissolved oceanic sulphate and phosphate. In: Fritz P, Fontes JC, editors. Handbook of environmental isotope geochemistry. Amsterdam: Elsevier; 1989. p. 219–255.
[14] Strauss H. Geological evolution from isotope proxy signals: sulfur. Chem Geol. 1999;161:89–101.
[15] Canfield DE. Biogeochemistry of sulfur isotopes. Rev Mineral Geochem. 2001;43:607–636.
[16] Seal RR II. Sulfur isotope geochemistry of sulfide minerals. Rev Mineral Geochem. 2006;61:633–677.
[17] Kroopnick P, Craig H. Atmospheric oxygen: isotopic composition and solubility fractionation. Science. 1972;175:54–55.
[18] Luz B, Barkan E. The isotopic composition of atmospheric oxygen. Global Biogeochem Cycles. 2011;25:GB3001.
[19] Epstein S, Mayeda T. Variation of O^{18} content of waters from natural sources. Geochim Cosmochim Acta. 1953;4:213–224.
[20] Craig H. Isotopic variations in meteoric waters. Science. 1961;133:1702–1703.
[21] Balci B, Shanks WC III, Mayer B, Mandernack KW. Oxygen and sulfur isotope systematics of sulfate produced by bacterial and abiotic oxidation of pyrite. Geochim Cosmochim Acta. 2007;71:3796–3811.
[22] Heidel C, Tichomirowa M. The role of dissolved molecular oxygen in abiotic pyrite oxidation under acid pH conditions – Experiments with ^{18}O-enriched molecular oxygen. Appl Geochem. 2010;25:1664–1675.
[23] Johnston DT, Farquhar J, Wing BA, Kaufman AJ, Canfield DE, Habicht KS. Multiple sulfur isotope fractionations in biological systems: a case study with sulfate reducers and sulfur disproportionators. Am J Sci. 2005;305:645–660.
[24] Kaplan IR, Rittenberg SC. Microbiological fractionation of sulphur isotopes. J Gen Microbiol. 1964;34:195–212.
[25] Sim MS, Bosak T, Ono S. Large sulfur isotope fractionation does not require disproportionation. Science. 2011;333:74–77.
[26] Antler G, Turchyn AV, Rennie V, Herut B, Sivan O. Coupled sulfur and oxygen isotope insight into bacterial sulfate reduction in the natural environment. Geochim Cosmochim Acta. 2013;118:98–117.
[27] Farquhar J, Canfield DE, Masterson A, Bao H, Johnston D. Sulfur and oxygen isotope study of sulfate reduction in experiments with natural populations from Faellestrand, Denmark. Geochim Cosmochim Acta. 2008;72:2805–2821.
[28] Fry B, Ruf W, Gest H, Hayes JM. Sulfur isotope effects associated with oxidation of sulfide by O_2 in aqueous solution. Chem Geol. 1988;73:205–210.
[29] Zerkle AL, Farquhar J, Johnston DT, Cox RP, Canfield DE. Fractionation of multiple sulfur isotopes during phototrophic oxidation of sulfide and elemental sulfur by a green sulfur bacterium. Geochim Cosmochim Acta. 2009;73:291–306.
[30] Cypionka H, Smock AM, Böttcher ME. A combined pathway of sulfur compound disproportionation in *Desulfovibrio desulfuricans*. FEMS Microbiol Lett. 1998;166:181–186.

[31] Habicht KS, Canfield DE, Rethmeier J. Sulfur isotope fractionation during bacterial reduction and disproportionation of thiosulfate and sulfite. Geochim Cosmochim Acta. 1998;62:2585–2595.
[32] Zerkle AL, Kamyshny A, Kump LR, Farquhar J, Oduro H, Arthur MA. Sulfur cycling in a stratified euxinic lake with moderately high sulfate: constraints from quadruple S isotopes. Geochim Cosmochim Acta.
[33] Richter A. Allgäuer Alpen. Berlin, Stuttgart: Gebr. Borntraeger; 1984.
[34] Canfield DE, Raiswell R, Westrich JT, Reaves CM, Berner RA. The use of chromium reduction in the analysis of reduced inorganic sulfur in sediments and shales. Chem Geol. 1986;54:149–155.
[35] Thode HG, Monster J, Dunford HB. Sulphur isotope geochemistry. Geochim Cosmochim Acta. 1961;25:159–174.
[36] Ono S, Wing B, Johnston D, Farquhar J, Rumble D. Mass-dependent fractionation of quadruple stable sulfur isotope system as a new tracer of sulfur biogeochemical cycles. Geochim Cosmochim Acta. 2006;70:2238–2252.
[37] Hulston JR, Thode HG. Variations in S^{33}, S^{34} and S^{36} contents of meteorites and their relation to chemical and nuclear effects. J Geophys Res. 1965;70:3475–3484.
[38] Farquhar J, Bao H, Thiemens M. Atmospheric influence of Earth's earliest sulfur cycle. Science. 2000;289:756–758.
[39] Strauss H. The isotopic composition of sedimentary sulfur through time. Palaeogeogr Palaeoclimat Palaeoecol. 1997;132:97–118.
[40] Hegler H, Lösekam-Behrens T, Hanselmann K, Behrens S, Kappler A. Influence of seasonal and geochemical changes on the geomicrobiology of an iron carbonate mineral water spring. Appl Environ Microbiol. 2012;78:7185–7196.
[41] Cortecci G, Dinelli E, Bencini A, Adorni-Braccesi A, La Ruffa G. Natural and anthropogenic SO_4 sources in the Arno River catchment, northern Tuscany, Italy: a chemical and isotopic reconnaissance. Appl Geochem. 2002;17:79–92.
[42] Johnston DT, Farquhar J, Canfield DE. Sulfur isotope insights into microbial sulfate reduction: When microbes meet models. Geochim Cosmochim Acta. 2007;71:3929–3947.
[43] Johnston DT, Farquhar J, Habicht KS, Canfield DE. Sulphur isotopes and the search for life: strategies for identifying sulphur metabolisms in the rock record and beyond. Geobiology. 2008;6:425–435.